PCP
PLANT & CELL PHYSIOLOGY

Regular Paper

Assembly Apparatus of Light-Harvesting Complexes: Identification of Alb3.1–cpSRP–LHCP Complexes in the Green Alga *Chlamydomonas reinhardtii*

Mithun Kumar Rathod[1,†], Sreedhar Nellaepalli[2,†], Shin-Ichiro Ozawa[3], Hiroshi Kuroda[2], Natsumi Kodama[2], Sandrine Bujaldon[4], Francis-André Wollman[4] and Yuichiro Takahashi[2,*]

[1]Graduate School of Natural Science and Technology, Okayama University, Okayama, 700-8530 Japan
[2]Research Institute for Interdisciplinary Science, Okayama University, Okayama, 700-8530 Japan
[3]Institute of Plant Science and Resources, Okayama University, Kurashiki, 710-0046 Japan
[4]Institut de Biologie Physico-Chimique, UMR7141 CNRS-Sorbonne Université, Paris 75005, France
[†]Equal contribution.

*Corresponding author: E-mail, taka@cc.okayama-u.ac.jp
(Received 19 June 2021; Accepted 30 September 2021)

The unicellular green alga, *Chlamydomonas reinhardtii*, contains many light-harvesting complexes (LHCs) associating chlorophylls *a*/*b* and carotenoids; the major LHCIIs (types I, II, III and IV) and minor light-harvesting complexes, CP26 and CP29, for photosystem II, as well as nine LHCIs (LHCA1–9), for photosystem I. A pale green mutant BF4 exhibited impaired accumulation of LHCs due to deficiency in the *Alb3.1* gene, which encodes the insertase involved in insertion, folding and assembly of LHC proteins in the thylakoid membranes. To elucidate the molecular mechanism by which ALB3.1 assists LHC assembly, we complemented BF4 to express ALB3.1 fused with no, single or triple Human influenza hemagglutinin (HA) tag at its C-terminus (cAlb3.1, cAlb3.1-HA or cAlb3.1–3HA). The resulting complemented strains accumulated most LHC proteins comparable to wild-type (WT) levels. The affinity purification of Alb3.1-HA and Alb3.1–3HA preparations showed that ALB3.1 interacts with cpSRP43 and cpSRP54 proteins of the chloroplast signal recognition particle (cpSRP) and several LHC proteins; two major LHCII proteins (types I and III), two minor LHCII proteins (CP26 and CP29) and eight LHCI proteins (LHCA1, 2, 3, 4, 5, 6, 8 and 9). Pulse-chase labeling experiments revealed that the newly synthesized major LHCII proteins were transiently bound to the Alb3.1 complex. We propose that Alb3.1 interacts with cpSRP43 and cpSRP54 to form an assembly apparatus for most LHCs in the thylakoid membranes. Interestingly, photosystem I (PSI) proteins were also detected in the Alb3.1 preparations, suggesting that the integration of LHCIs to a PSI core complex to form a PSI–LHCI subcomplex occurs before assembled LHCIs dissociate from the Alb3.1–cpSRP complex.

Keywords: Affinity purification • ALB3.1 • *Chlamydomonas reinhardtii* • Light-harvesting complex • Photosystem • Thylakoid membranes

Introduction

Capture of light energy by photosynthetic pigments is the initial step of photosynthesis reactions. In plants and green algae, there are two types of light-harvesting apparatus: core and peripheral antenna complexes. The core antenna complexes associate with photosystem I (PSI) and photosystem II (PSII) core complexes that are mainly composed of intrinsic proteins encoded by chloroplast genes. The peripheral antenna complexes consist of light-harvesting chlorophyll-binding proteins (LHCPs), which bind chlorophyll *a* (Chl *a*), chlorophyll *b* (Chl *b*) and carotenoid molecules. The LHCPs are encoded by two multigenic gene families in the nucleus and form light-harvesting complexes (LHCs) in the thylakoid membranes. The *lhca* genes encode LHCI proteins that associate with the PSI core complex to form a PSI–LHCI supercomplex (Ben-Shem et al. 2003, Ozawa et al. 2018), whereas the *lhcb* genes code for LHCII proteins that mainly bind to the PSII core complex to form a PSII–LHCII supercomplex (Sheng et al. 2021). Excitation energy trapped by LHCs is transferred to the core antenna complexes and is finally used for photochemical reactions in PSI and PSII reaction centers (RCs).

LHCPs are integral proteins with three transmembrane helices (TM1–3) and are the most abundant proteins in the thylakoid membranes. LHCPs are translated in the cytosol as precursor proteins with an N-terminal chloroplast transit peptide (TP) and are translocated to and integrated into the thylakoid membranes (Richter et al. 2010, Dall'Osto et al. 2015, Ziehe et al. 2017, 2018). The TP is used to direct the precursor proteins into the chloroplast by translocating across the envelope membranes via the translocon at the outer envelope membrane of chloroplasts (TOC) and translocon at the inner envelope membrane of chloroplasts (TIC) complexes translocon. Upon translocation, the TP is cleaved off by a stromal processing peptidase and the resulting mature proteins form a transit complex

Plant Cell Physiol. 63(1): 70–81 (2022) doi:https://doi.org/10.1093/pcp/pcab146, Advance Access publication on 1 October 2021, available online at https://academic.oup.com/pcp

with the chloroplast signal recognition particle (cpSRP). The translocation of LHCPs from the TIC/TOC translocon to cpSRP is mediated by the LHCP translocation defect (LTD) protein (Ouyang et al. 2011, Jeong et al. 2018). The formation of the cpSRP–LHCP complex allows the hydrophobic LHCPs to remain soluble in the stroma and prevents their aggregation.

In vascular plants, the cpSRP consists of a heterodimer of cpSRP43 and cpSRP54. The cpSRP54 is an ortholog of the cytosolic and prokaryotic SRP54 (Dunschede et al. 2015). Although SRP54 contains a conserved RNA, cpSRP54 lacks the RNA and instead recruited cpSRP43 (Ziehe et al. 2017). In vitro assay using synthetic peptides suggested that cpSRP43 binds LHCPs through the L18 region located between the two TM helices, TM2 and TM3, of LHCPs, whereas no significant interaction between cpSRP54 and LHCPs is observed (DeLille et al. 2000, Tu et al. 2000, Stengel et al. 2008). In Arabidopsis, cpSRP43 is sufficient for forming a soluble cpSRP43–LHCP complex in the stroma (Tu et al. 2000, Dunschede et al. 2015), while the integration of LHCPs into the thylakoid membranes requires cpSRP54, cpFtsY, Alb3 and guanosine triphosphate (GTP).

The cpSRP–LHCP complexes are directed to the thylakoid membranes via the cpSRP receptor cpFtsY peripherally bound to the thylakoid membranes. Both cpFtsY and cpSRP54 contains a GTP binding and hydrolysis domain (Ziehe et al. 2018). Finally, the LHCPs are inserted into the thylakoid membranes by Albino 3 (Alb3) (Sundberg et al. 1997). Alb3 is a chloroplast homolog of the mitochondrial Oxa1p and *Escherichia coli* YidC, which are essential for integrating membrane proteins in membranes. Alb3 has five putative TM helices and is present in the thylakoid membranes.

The green algae also contain LTD, cpSRP43, cpSRP54, CpFtsY and Alb3 (Ziehe et al. 2017). The green alga *Chlamydomonas reinhardtii* is an excellent model organism for studying the assembly of the LHCs because all the lhc genes and LHCPs have been identified and a variety of LHC-deficient mutants is available. In particular, mutants deficient in LTD (Jeong et al. 2018), cpSRP43 (Kirst et al. 2012b, Bujaldon et al. 2020), cpSRP54 (Jeong et al. 2017) and cpFtsY (Kirst et al. 2012a) have been isolated and characterized. These mutants, except for the cpSRP54 mutant, are pale green and contain significantly reduced levels of LHCPs. The cpSRP54 mutant shows a milder pale green phenotype and accumulates more LHCPs than the other mutants, suggesting that the cpSRP54 is less important for the assembly of LHCs (Jeong et al. 2017). *C. reinhardtii* contains two Alb3 proteins, Alb3.1 and Alb3.2. Alb3.1 is required for the accumulation of LHCPs (Bellafiore et al. 2002, Bujaldon et al. 2020), whereas Alb3.2 appears to have a wider role than Alb3.1 and is also required for the accumulation of PSI and PSII complexes and is essential for cell survival (Gohre et al. 2006). Alb3.1 and Alb3.2 are located in the thylakoid membranes and are associated with a large complex. In addition, coimmunoprecipitation experiments suggested that these two proteins interact directly or indirectly with each other (Gohre et al. 2006).

In a previous study, we reported that the pale green mutant BF4 is defective in the *ALB3.1* gene and accumulates the LHCPs at <25% of WT levels and concluded that Alb3.1 is essential for proper LHCP assembly in the thylakoid membranes (Bujaldon et al. 2020). In the present study, we complemented BF4 with vectors that express Alb3.1, Alb3.1-HA (Alb3.1 fused with a single HA tag at the C-terminus) or Alb3.1–3HA (Alb3.1 fused with a triple HA tag at the C-terminus) and confirmed that these complemented strains accumulate LHCPs at nearly WT levels. To further elucidate how Alb3.1 assists the assembly of LHCs in the thylakoid membranes, we purified Alb3.1-HA and Alb3.1–3HA from the thylakoid membrane extracts by affinity spin column to identify interacting proteins. The purification and characterization of HA-tag fused Alb3.1 reveal an intimate interaction of cpSRP43, cpSRP54 and many LHCI and LHCII proteins with Alb3.1. We conclude that LHCs are assembled in the thylakoid membranes by the formation of a transient assembly apparatus of Alb3.1–cpSRP–LHCP complexes. We also suggest that the Alb3.1–cpSRP–LHCP complexes transiently associate an assembly intermediate of the PSI–LHCI supercomplex.

Results

Complementation of BF4 with Alb3.1 cDNA

The pale green BF4 mutant cells grow photoautotrophically but accumulate light-harvesting chlorophyll-binding proteins (LHCPs) at about 20% of the WT level (Bujaldon et al. 2020). This mutant is defective in the insertase Alb3.1. To address the molecular mechanism by which LHCs are assembled in the thylakoid membranes, we complemented the BF4 mutant with three different complementation vectors to express Alb3.1, Alb3.1-HA or Alb3.1–3HA from the *ALB3.1* cDNA driven by the *PSAD* promoter/terminator (**Fig. 1A**). After the introduction of one of these vectors into BF4 cells by electroporation as described in the 'Materials and Methods' section, putative transformants were selected on agar plates containing paromomycin as shown in Supplementary Figure. When transformed with the vector expressing Alb3.1–3HA, the color of the cells on agar plates is variable as shown in Supplementary Figure; some are as green as WT, some are pale green like BF4 and the others are intermediates. The clones as green as the WT were selected for further analysis. The total cellular DNA was isolated and used as a template to amplify the insertion of the transforming vector, and the resulting DNA fragments were analyzed by agarose gel electrophoresis (**Fig. 1B**). No band is detected in WT and BF4 as expected, whereas DNA fragments of 135 bp, 162 bp and 216 bp are amplified in the three complemented strains, cAlb3.1, cAlb3.1-HA and cAlb3.1–3HA, respectively, indicating that the introduction of the complementation vectors to the nuclear genome is successful. Since antibody against Alb3.1 is not available, Alb3.1-HA and Alb3.1–3HA were detected using anti-HA antibody. A weak signal of Alb3.1-HA is detected around 50 kDa in Alb3.1-HA cells, while a strong signal of a slightly larger size is detected in Alb3.1–3HA cells (**Fig. 1C**). The strong signal of Alb3.1–3HA may be ascribed to the fact that the anti-HA antibody reacted more

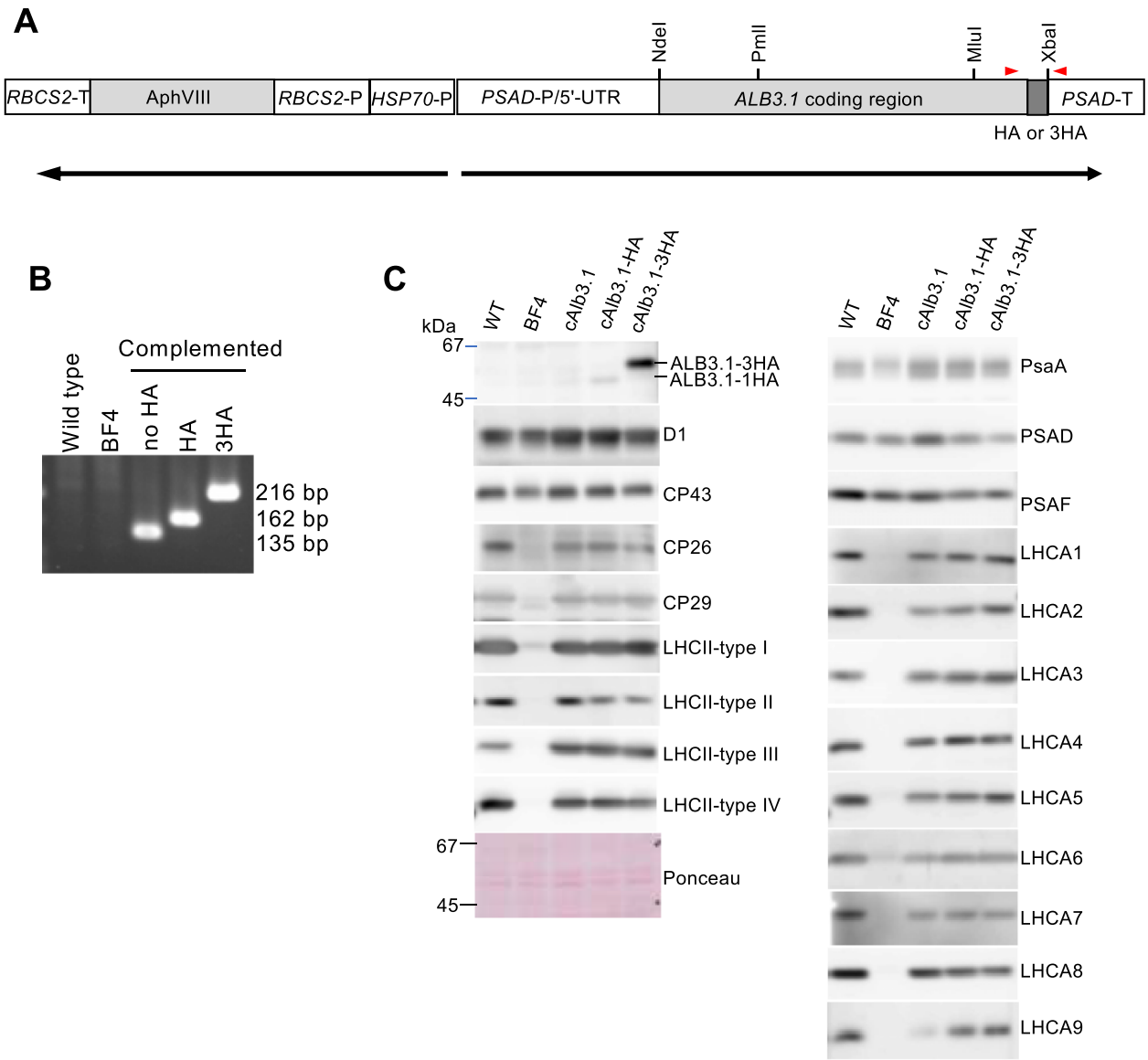

Fig. 1 Complementation of BF4 cells. (A) Physical map of the transformation vector. ALB3.1 coding region amplified from the cDNA library is under the control of the promoter/5′-UTR and terminator of *Chlamydomonas* PSAD (PSAD-P/5′-UTR and PSAD-T, respectively). Coding regions of a single HA or a triple HA tag is inserted at the coding region of the C-terminus of ALB3.1. The vector carries a selectable paromomycin resistance gene (AphVIII) under the control of the HSP70 promoter (HSP70-P), RBCS2 promoter (RBCS2-P) and RBCS2 terminator (RBCS2-T). Restriction sites (*Nde*I, *Pml*I, *Mlu*I and *Xba*I) used for plasmid construction are also shown. Arrows indicate the orientation of the genes. Red arrowheads represent primers used for PCR. (B) Confirmation of the insertion of the HA tag coding region in the complemented strains by the chimeric ALB3.1 transgene without HA (no HA) or with a single or a triple HA (HA and 3-HA). WT and BF4 strains, which lack the chimeric ALB3.1 transgene, were used as negative controls. PCR was carried out as described in the 'Materials and Methods' section. Estimated sizes of the PCR products are shown. (C) Accumulation of PSI, LHCI and LHCII proteins in WT, BF4 and complemented BF4 (cAlb3.1, cAlb3.1-HA and cAlb3.1−3HA) cells. Total cell proteins (0.5 μg Chl but 0.1 μg Chl for BF4) were solubilized with 2% (w/v) SDS and 0.1 M DTT at 100°C for 1 min and protein extracts were separated by SDS-PAGE, electroblotted onto a nitrocellulose filter, probed with specific antibodies against HA tag, PSII proteins (D1 and CP43), LHCII proteins (CP26, CP29 and LHCII-types I–IV), PSI proteins (PsaA, PSAD and PSAF) and LHCI proteins (LHCA1-9).

intensively with the triple HA tag than with the single HA tag of Alb3.1-HA. Although the BF4 cells accumulate LHCI and LHCII proteins at significantly reduced levels, as reported previously (Bujaldon et al. 2020), the three complemented strains have restored the accumulation of LHCI and LHCII proteins; LHCI proteins accumulate to substantial levels but to slightly decreased levels compared with those in WT cells, while LHCII proteins to nearly WT levels (**Fig. 1C**). The similar amount of LHCI and LHCII proteins in the three complemented strains indicates that the fusion of the single or triple HA tag at the

C-terminus of Alb3.1 does not significantly affect its ability to contribute to the membrane insertion and accumulation of LHC proteins.

Alb3.1 associates with cpSRP43 and cpSRP54

To identify proteins interacting with Alb3.1, HA-tagged Alb3.1 was used as bait, and proteins interacting with Alb3.1 were isolated by affinity spin columns. Since Alb3.1 is localized in the thylakoid membranes, we isolated the thylakoid membranes from cAlb3.1-HA and cAlb3.1–3HA strains, solubilized them with *n*-dodecyl-α-D-maltoside (α-DDM), and applied the resulting extracts to affinity spin columns. As a negative control, the thylakoid extracts from WT cells were used. The purified preparations were incubated with sodium dodecyl sulfate (SDS) and dithiothreitol, and the solubilized polypeptides were separated by SDS-polyacrylamide gel electrophoresis (SDS-PAGE) and stained with silver (**Fig. 2A**). The preparation from WT as a negative control shows several polypeptides in a high-molecular region (>60 kDa), which are nonspecific contaminations. The strong band below the 66 kDa marker protein was identified as AtpA (the α-subunit of chloroplast ATP synthase) by mass spectrometry analysis, the intensity of which differs from preparation to preparation. A more complex and quite similar polypeptide pattern was observed in the Alb3.1-HA and Alb3.1–3HA preparations. The most significant difference between the two Alb3.1 preparations was found in the 45–66 kDa region (marked with asterisks in **Fig. 2A**). To further characterize the Alb3.1 preparations, we performed large-scale purifications and separated their polypeptides by two different SDS-PAGE systems, a Tris–HCl resolving gel buffer system (Laemmli 1970) (**Fig. 2B**) and a urea–2-morpholinoethanesulfonic acid (MES) Tris resolving gel buffer system (Kashino et al. 2001), which better separates LHCI polypeptides from LHCII polypeptides (**Fig. 2C**). The polypeptides of these preparations were also compared with the polypeptides of LHCII and PSI–LHCI preparations from WT cells, shown on the left side of **Fig. 2A**. The comparison of the polypeptides from LHCII and PSI–LHCI complexes with those from the Alb3.1 preparations suggests that the Alb3.1 preparations contain several LHCI and LHCII polypeptides.

Next, the separated polypeptides (bands 1–19) were digested with trypsin and were subjected to liquid chromatography–tandem mass spectrometry (LC–MS/MS) for sequence identification of their peptide profile. The band 2/3 in the Alb3.1-HA preparation and the band 2 in the Alb3.1–3HA preparation in **Fig. 2B**, which correspond to the bands marked by asterisk in **Fig. 2A**, contain Alb3.1-HA and Alb3.1–3HA, respectively, as well as AtpA (**Table 1**). The relative migration of the two Alb3.1 bands well corresponds to signals detected with anti-HA antibody as shown in **Fig. 1C**. The difference in size is ascribed to the number of HA tag fused at the C-terminus of Alb3.1. The band 3 of the Alb3.1–3HA preparation and the band 2/3 of the Alb3.1-HA preparation contain cpSRP54 (**Fig. 2B** and **Table 1**). Band 4 detected in both Alb3.1-HA and Alb3.1–3HA

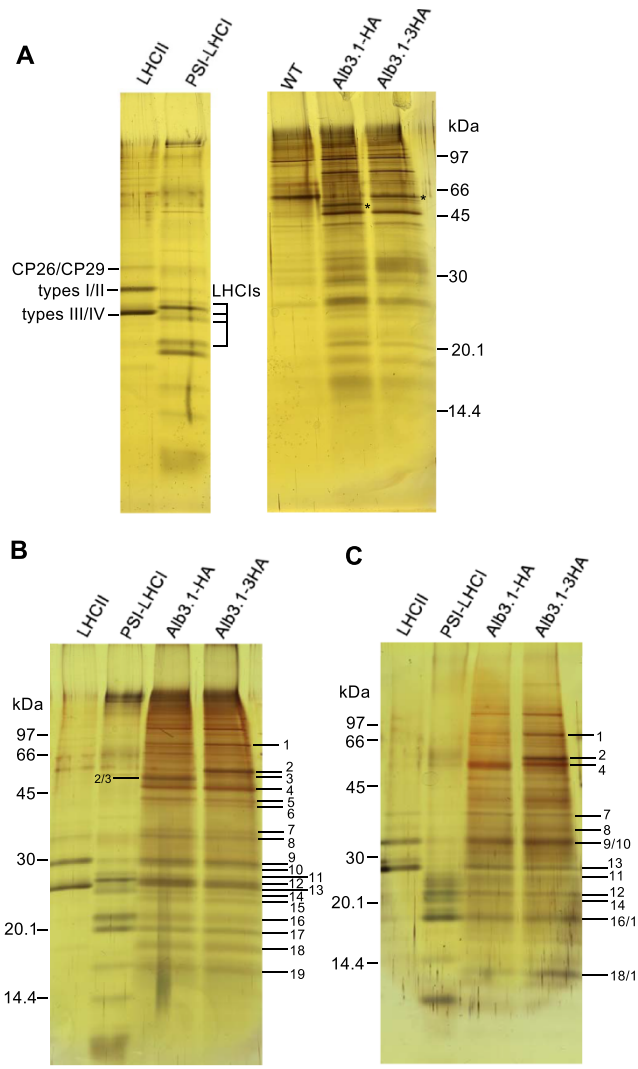

Fig. 2 Polypeptide profiles of the affinity purified Alb3.1 preparation. (A) Comparison of the polypeptides of affinity-purified preparations from WT, Alb3.1-HA and Alb3.1–3HA. The thylakoid membranes were solubilized with 1% α-DDM, and Alb3.1 preparations were purified by affinity spin column as described in the 'Materials and Methods' section. The samples were solubilized with 2% (w/v) SDS and 0.1 M DTT at 80°C for 1 min and protein extracts were separated by SDS-PAGE and the gels were stained with silver. For further characterization of the polypeptides of the Alb3.1 preparations, the polypeptides were separated by two SDS-PAGE systems; (B) Laemmli system and (C) urea–MES–Tris system. The polypeptides of the preparations were also compared with the polypeptides of LHCII and PSI–LHCI preparations from WT cells. The polypeptides marked by numbers were subjected to trypsin digestion, and the resulting digests were analyzed by LC–MS/MS. The assignments of these polypeptides are summarized in **Table 1**.

preparations is assigned to cpSRP43. To confirm that cpSRP54 and cpSRP43 are exclusively present in Alb3.1 preparations, we analyzed the presence of Alb3.1, cpSRP54 and cpSRP43 in the negative control lane. Six gel slices from the region between 45 and 66 kDa marker proteins were cut and analyzed with

Table 1 Identification of polypeptides in the Alb3.1-HA and Alb3.1–3HA preparations. The polypeptides of the Alb3.1-HA and Alb3.1–3HA were separated by SDS-PAGE and stained with silver as shown in **Fig. 2** (panels B and C). The polypeptides in the gel (bands 1–20) were excised and digested with trypsin, and the resulting polypeptides were applied to LC–MS/MS. Assigned peptide sequences, position of the identified peptides in the protein sequence (position), and the score for assigned polypeptide sequence (Xcorr) are shown. Bold M represents methionine sulfoxide (monooxidized methionine)

Band	Transcript gene ID accession ID	Protein name	Assigned peptide sequence	Position	Xcorr
1	Not identified				
2	Cre06.g251900.t1.2	Alb3.1	QQVESAMAVQALKPR	84–98	4.49
			KLGGANVV**M**NELGPVTKPGSGR	280–301	4.54
			LGGANVV**M**NELGPVTKPGSGR	281–301	3.72
			NGVAAGEWSVWKPATVLTTAEAAK	303–326	4.87
			ARAEAEEAVER	327–337	4
	Q96550	AtpA	G**M**ALNLQADHVGVVVFGNDSLIHQGDLVYR	124–153	4.65
			EVAAFAQFGSDLDAATQYVLER	462–483	3.24
3	Cre11.g479750.t1.2	cpSRP54	VLEGVTPDVQFIK	129–141	3.48
			TVSNELIDLMGGGTGAK	142–158	5.13
			TVSNELIDL**M**GGGTGAK	142–158	4.38
			SAVRPSDTLLVVDAMTGQEAANLVR	274–298	4.74
			SFNEAVDISGAILTK	299–313	4.81
			ANSLLQELVASAGK	509–522	4.16
4	Cre04.g231026.t1.1	cpSRP43	WKDGSDSTWEVAADLSEDLVR	88–108	3.81
			SALHFAAALGSAECTR	147–162	4.4
			EGYTPLHMAAGYMHTPSMAVLLEAGANPEIK	177–207	3.85
			LYDEVEPGNVLNCR	249–262	4.14
			NVSADVLEDYLAGLEYAVAEEVLDVVQVR	289–317	5.35
5	P10898	PsbC	VITNPTTNAAVIFGYLVK	186–203	5.27
			LGANVASAQGPTGLGK	312–327	4.25
			SPTGEIIFGGET**M**R	332–345	3.65
			AAEY**M**THAPLGSLNSVGGVATEINAVNFVSPR	380–411	3.74
6	Cre07.g346050.t1.2	CRD1 Magnesium-protoporphyrin IX monomethyl ester (oxidative) cyclase, chloroplastic, Cupper response defect 1 protein	FYTTDFDEMEQLFSK	68–82	4.46
			FYTTDFDE**M**EQLFSK	68–82	4.09
			ASSPEVAEMFLLMSR	157–171	3.54
			ASSPEVAEMFLL**M**SR	157–171	3.68
			ALSDFNLALDLGFLTK	183–198	6.16
			FIIYATFLSEK	209–219	3.91
			FYESLGLNTR	302–311	3.62
			LVELSASSSPLAGLQK	354–369	4.93
			EKDVGSVDIAGSGASR	388–403	3.65
			DVGSVDIAGSGASR	390–403	5.02
7	P23577	PetA	VGNLYYQPYSPEQK	128–141	3.62
			SNNTIYNASAAGK	197–209	3.99
			EGQTVQADQPLTNNPNVGGFGQAETEIVLQNPAR	249–282	6.35
8	Cre16.g673650.t1.1	LHCB5 (CP26)	GWLGGQGGAADLDK	38–51	4.5
			KLFLPSGLYDR	58–68	3.13
			NGTGPAGYSPGIGK	185–198	3.66
			HVADPFGYNLLTVLGAEER	267–285	5.73
			LA**M**VSVLGFAVQSYVTGEGPYANWTK	241–266	4.89
	Cre17.g720250.t1.2	LHCB4 (CP29)	GSVEAIVQATPDEVSSENR	102–120	5.99
			LAPYSEVFGLAR	121–132	3.14
9	Cre04.g232104.t1.1	LHCBM3 (Type I)	QAPASSGIEFYGPNR	31–45	3.42
			YRELELIHAR	86–95	3.58
			AGAQIFSEGGLDYLGNPSLVHAQNIVATLAVQVILMGLVEGYR	125–167	4.13
			AGAQIFSEGGLDYLGNPSLVHAQNIVATLAVQVIL**M**GLVEGYR	125–167	5.28
10	Not identified				
11	Cre10.g452050.t1.2	LHCA4	WYAQAEL**M**NAR	95–105	3.02
			YQDFVKPGSANQDPIFTNNK	165–184	4.64

(continued)

Table 1 (Continued)

Band	Transcript gene ID accession ID	Protein name	Assigned peptide sequence	Position	Xcorr
12	Cre11.g467573.t1.1	LHCA3	SKDQLYVGASQSSLAYLDGSLPGDFGFDPLGLLDPVNSGGFIEPK	41–85	5.48
	Cre06.g278213.t1.1	LHCA6	EVESPLGPLGLLAVEFFL**M**HWVEVR	103–127	3.71
			KPGSVDQDPIFSQYK	134–148	2.64
13	Cre12.g548400.t1.2	LHCBM2 (Type III)	YRELELIHAR	78–87	3.58
			AGAQIFAEGGLNYLGNENLIHAQSIIATLAFQVVVMGLAEAYR	117–159	4.57
			AGAQIFAEGGLNYLGNENLIHAQSIIATLAFQVVV**M**GLAEAYR	117–159	5.22
			ANGGPLGEGLDPLHPGGAFDPLGLADDPDTFAELK	160–194	4.7
			LAMFSMFGFFVQAIVTGK	203–220	4.76
			GPIQNLDDHLANPTAVNAFAYATK	221–244	3.91
14	Cre06.g272650.t1.2	LHCA8	YATGAGPVDNLAAHLK	211–226	3.14
15	Cre12.g550850.t1.2	PSBP1	YEDNFDAVNNLVVIAQDTDKK	106–126	3.62
			QAYSGETQSEGGFAPNR	148–164	4.83
			VSAASLLDVSTTTDKK	165–180	4.18
			HQLIGATVGSDNK	202–214	3.68
16	Cre06.g283050.t1.2	LHCA1	FTESEVIHGR	74–83	3.73
			GDAGGVVYPGGAFDPLGFAK	146–165	3.89
	Cre07.g344950.t1.2	LHCA9	TQPIEGLTAHLADPFGK	181–197	2.96
			NITYYLTHLPETLGSA.[-]	198–213	2.52
17	Cre09.g412100.t1.2	PSAF	LKQYEADSAPAVALK	91–105	5.05
			QYEADSAPAVALK	93–105	3.15
			GTLLEKEENITVSPR	213–227	4.27
18	Cre12.g558900.t1.2	PETO	KAEVVESTSGGLDPR	101–115	3.09
			SVALPGALALTIGGFVAASK	116–135	4.12
			DSNNYAGYEATLK	151–163	3.62
19	Not identified				
20	Not identified				

LC–MS/MS. This region of the gel may possibly contain Alb3.1, cpSRP54 and cpSRP43, but no peptides of Alb3.1, cpSRP54 and cpSRP43 were detected except for the peptides of AtpA and AtpB, which were also detected in the Alb3.1 preparations (see **Table 1**). Thus, cpSRP54 and cpSRP43 are exclusively associated with Alb3.1. CpSRP54 and cpSRP43 form the cpSRP complex and are mainly present in the stroma as a soluble complex (Ziehe et al. 2018). However, the present finding reveals that part of cpSRP is associated with Alb3.1 and is thus bound to the thylakoid membranes. It is of note that the amount of cpSRP54 is much lower than that of cpSRP43 in the Alb3.1 preparations, based on the staining intensities on the gels. Although it has already been reported by in vitro experiments that cpSRP has an affinity with Alb3.1 (Lewis et al. 2010, Dunschede et al. 2011), the present study indicates that Alb3.1 and cpSRP interact in the thylakoid membranes strongly enough to resist the solubilization of the thylakoid membranes with α-DDM.

It is of interest that magnesium-protoporphyrin IX monomethyl ester cyclase, which is involved in chlorophyll synthesis, is also detected in the band 6. However, the thylakoid membrane-associated SRP receptor, cpFtsY, and Ab3.2 are not detected in these experiments.

Alb3.1 associates with LHCPs

The Alb3.1-HA and Alb3.1–3HA preparations contain several polypeptides, the relative electrophoretic migrations of which correspond to those of LHCI and LHCII polypeptides (**Fig. 2B**, **C**). LC–MS/MS analysis reveals that, apart from band 10, bands 8–16 contain peptides from LHC proteins (**Table 1**). Band 8 is assigned to minor LHCIIs, CP26 and CP29, which are not separated as discrete bands under the present electrophoresis conditions. Bands 9 and 13 are assigned to LHCII types I and III, respectively, but LHCII types II and IV were not detected. In addition, six LHCI proteins, LHCA4, LHCA3/LHCA6, LHCA8 and LHCA1/LHCA9 are assigned to bands 11, 12, 14 and 16, respectively. In addition to these LHCPs, some proteins localized in the thylakoid membranes are detected: PSAF of PSI (band 17), PsbC (CP43) and PSBP1 of PSII (bands 5 and 15), PetA (Cyt f) and PETO of Cyt b_6f (bands 7 and 18) and AtpA of ATP synthase (band 2) (**Table 1**). It remains to be determined whether these are specifically associated with Alb3.1, but it is highly likely that AtpA is a nonspecific contamination because this protein is detected in the negative control sample as well.

Immunological identification of proteins in the Alb3.1–3HA preparation

The polypeptides from the Alb3.1–3HA were also analyzed by immunoblotting. When probed with anti-HA antibody, a very strong signal is detected in the Alb3.1–3HA preparation, indicating that the Alb3.1–3HA is significantly enriched in the preparation, as expected (**Fig. 3**). The anti-LHCII antibody, which reacts with major LHCII proteins (LHCII types I–IV), detected the signals corresponding to LHCII types I and III but did not detect LHCII types II and IV, which is consistent with the results by LC–MS/MS analyses. Probing with an anti-LHCII type I antibody, which reacts with both LHCII type I and CP29, reveals

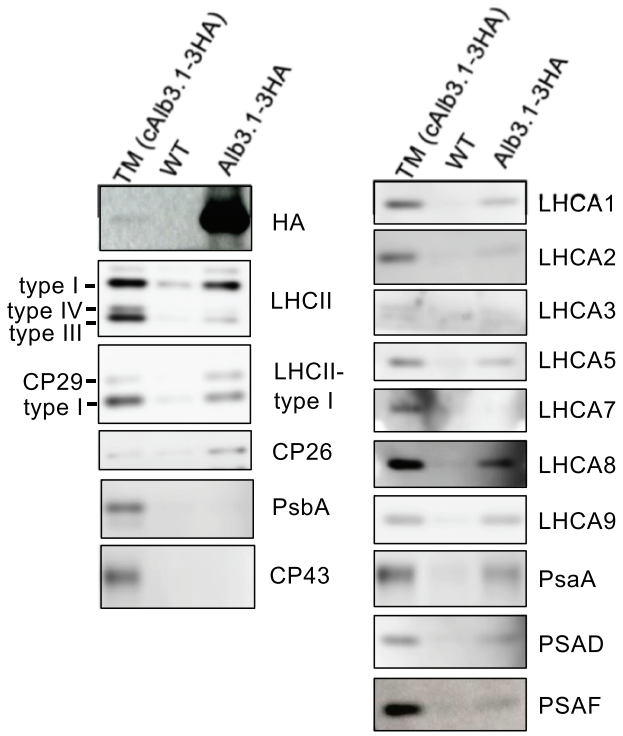

Fig. 3 Identification of the interacting proteins with Alb3.1 by immunoblotting. The affinity purified preparations from WT and Alb3.1–3HA thylakoid extracts as well as the thylakoid membranes from cAlb3.1–3HA (TM) were solubilized with 2% (w/v) SDS and 0.1 M DTT at 80°C for 1 min and protein extracts were separated by SDS-PAGE, electroblotted onto a nitrocellulose filter and probed with specific antibodies raised against LHCI, LHCII, PSI and PSII proteins. Alb3.1–3HA was detected with the anti-HA antibody.

that these two proteins are present. In addition, the presence of CP26 is confirmed immunologically. Although faint bands of CP26 and LHCII type I were detected in the preparation from the WT thylakoid extracts, the intensity of the signals was significantly weaker than those of the corresponding signals in the Alb3.1 preparation. Thus, LC–MS/MS and immunoblot analyses confirmed the presence of LHCII proteins except for LHCII types I and IV in the Alb3.1–3HA preparation. Immunoblot analyses also detected several LHCI proteins: LHCA1, 2, 5, 8 and 9 but not LHCA7. Since the activity of the antibodies against LHCA3, LHCA4 and LHCA6 is rather weak, it proved difficult to confirm the presence of either of these three LHCI proteins, although LC–MS/MS detected peptides from their sequence (**Table 1**). We noted that the immunoblots revealed the presence of the three photosystem I (PSI) proteins, PsaA, PSAD and PSAF but not the presence of PSII proteins, PsbA (D1) and PsbC (CP43). It is unlikely that Alb3.1 is required for the insertion of PsaA, which has 11 TM helices, into the thylakoid membranes, because PsaA is encoded by the chloroplast *psaA* gene, and the PSI complex is properly assembled in BF4 mutant cells as we reported previously (Bujaldon et al. 2020) and as documented in **Fig. 1**. Although PSAD, which is peripherally located on the stromal side of the PSI RC complex, and PSAF, which has one TM helix with which the most hydrophilic region located on the lumenal side of the PSI RC complex, are encoded by nuclear genes, the BF4 mutant cells also accumulated these two proteins. Thus, we suspect that their interaction of the PSI proteins with Alb3.1 is indirect as will be discussed below.

Alb3.1 transiently associates newly synthesized LHCII proteins

The cpSRP pathway suggests that the cpSRP–Alb3.1 complex transiently associates with newly synthesized LHCPs. To address this question, we isolated an Alb3.1 preparation from cells that were radiolabeled with ^{35}S. **Fig. 4** shows the fluorography of the labeled polypeptides of the thylakoid membranes and the purified Alb3.1 preparation separated by a longer gel for a better resolution. The pulse-labeled polypeptides of the thylakoid membranes showed heavily labeled bands corresponding to PSII proteins (CP47/CP43 and D1/D2) and sharp bands of LHCII types I/II and III/V. CP26 and CP29 migrated in the same region as D1 under the present electrophoresis conditions. The labeling of LHCI proteins was much weaker, as expected from their much lower content in the thylakoid membranes when compared with LHCII proteins (Ozawa et al. 2010). During the 4-h chase period, the intensity of PSII proteins becomes weaker because they turnover rapidly, whereas the intensity of the signal of LHCPs remains almost constant.

Many pulse-labeled polypeptides were also detected in the Alb3.1 preparation. Pulse-labeled bands in the 45–60-kDa region appear to correspond to Alb3.1-HA, cpSRP54 and cpSRP43, and these signals are stable during the chase experiment. The sharp band due to AtpA is also detected above the Alb3.1-HA under the present electrophoresis conditions. In addition, we detected several labeled LHCII proteins: LHCII type I (LHCII-I) and type III (LHCII-III) as well as CP26/CP29. The intensity of these signals significantly decreases during chase experiments. We hardly detected any labeled LHCI proteins in line with their lower labeling in the thylakoid membranes. The decreased labeling of LHCII proteins upon 4-h chase experiments is consistent with the fact that the newly synthesized LHCII proteins transiently associate with the cpSRP–Alb3.1 complex, while they insert into the thylakoid membranes.

Discussion

Alb3.1 has a stable interaction with cpSRP

In vascular plants, cpSRP43 and cpSRP54 form a heterodimer complex, and the cpSRP binds LHC apoproteins in the stroma (Aldridge et al. 2009, Horn et al. 2015, Ziehe et al. 2018). The L18 motif located between the second and third TM helices of LHCP binds to the ankyrin repeats of cpSRP43 (Tu et al. 2000, Stengel et al. 2008, Horn et al. 2015). The C-terminal ARRKR motif of cpSRP54 binds to the C-terminal chromodomain 2

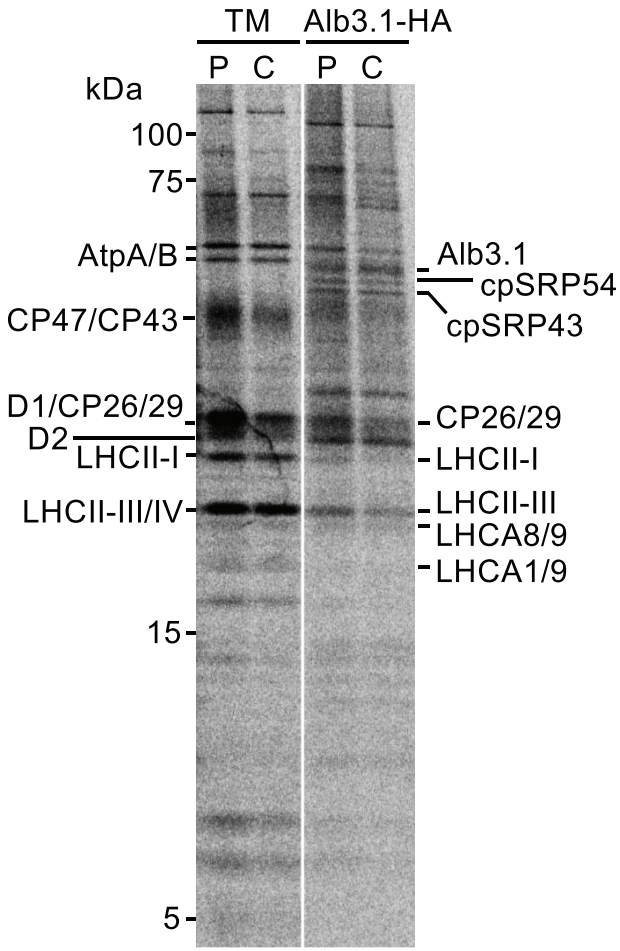

Fig. 4 Transient association of LHCPs in the Alb3.1 preparation. Total cellular proteins from cAlb3.1-HA cells were labeled with 5 μCi/ml $Na_2{}^{35}SO_4$ for 20 min (P) and chased for 4 h (C). TM, thylakoid membranes; Alb3.1-HA, Alb3.1-HA preparation.

(CD2) of cpSRP43 (Richter et al. 2010, Horn et al. 2015). The cpSRP–LHC complex is transported as a stroma-soluble transient complex to the thylakoid membranes where LHC apoproteins are membrane-integrated with the assistance of Alb3. Thus, it is inferred that cpSRP is mainly present in the stroma and only transiently binds to Alb3 in the thylakoid membranes. The crystal structure of the cpSRP43–A3CT (Alb3 C-terminal tail) complex revealed that two positively charged motifs in the A3CT binds to the C-terminal chromodomain 3 (CD3) of cpSRP43 (Horn et al. 2015). In green algae, the twin arginine of the ARRKR motif is conserved in cpSRP54 but the alanine is replaced by valine, which has a bulkier side chain that may sterically prevent the interaction with cpSRP43 (Dunschede et al. 2015). Also, some critical amino acid residues in the CD2 domain are not conserved in cpSRP43, which may alter the cpSRP43–cpSRP54 interaction (Dunschede et al. 2015). Actually, yeast-two-hybrid, in vitro pulldown experiments and size-exclusion chromatography separation of total protein extracts from *Chlamydomonas* cells revealed that cpSRP54 and cpSRP43 do not form a complex (Dunschede et al. 2015). However, we found in the present study that the purified Alb3.1 preparations contain both cpSRP43 and cpSRP54, although the amount of cpSRP54 appears lower than that of Alb3.1 and cpSRP43 (**Fig. 2** and **Table 1**).

Thus, our finding indicates that at least part of cpSRP43 and cpSRP54 associates with Alb3.1 in the thylakoid membranes. It is inferred that the interaction between Alb3.1 and cpSRP43/cpSRP54 may be transient but that it is rather stable since it resisted solubilization with the detergent. The presence of both cpSRP43 and cpSRP54 in the Alb3.1 preparations suggests that either these two factors interact as a cpSRP in the Alb3.1 preparations or that they bind to Alb3.1 individually. The Chlamydomonas truncated light-harvesting antenna 4 mutant, which has a lesion of the *cpSRP54* gene, showed a pale green phenotype and a reduced accumulation of LHCPs (Jeong et al. 2017). However, it accumulated more LHCPs than the *tla3* and *p71* mutants deficient in cpSRP43 (Kirst et al. 2012b, Bujaldon et al. 2020), the *tla2* mutant deficient in cpFtsY (Kirst et al. 2012a) and the *ac29-3* and BF4 mutants deficient in Alb3.1 (Bellafiore et al. 2002, Bujaldon et al. 2020). These results argue for a more limited role of cpSRP54 in the accumulation of LHCPs as compared to that of the other biogenesis factors in *C. reinhardtii*. Our present finding that a smaller amount of cpSRP54 than of cpSRP43 is present in the Alb3.1 preparations further supports this view.

It was reported that the solubilized Alb3.1 is found in two complexes of 100–150 and 600–700 kDa (Bellafiore et al. 2002). The apparent molecular mass of the smaller complex may be a dimer of Alb3.1, but the large complex is much larger than what would be expected for Alb3.1–cpSRP. This observation suggests that the cpSRP43–Alb3.1 complex may associate with additional proteins. However, cpFtsY, the receptor protein of cpSRP, which is peripherally bound to the thylakoid membranes, is not detected in the Alb3.1 preparation. A reciprocal immunoprecipitation experiments suggested that Alb3.1 forms a complex with Alb3.2, which is the homolog of Alb3.1 and is also present in the thylakoid membranes (Gohre et al. 2006). However, we did not find Alb3.2 in the Alb3.1 preparations. Instead, we detected the magnesium-protoporphyrin IX monomethyl ester (oxidative) cyclase, which catalyzes the reaction to convert porphyrin to chlorine in the chlorophyll biosynthesis pathway. That the enzyme involved in chlorophyll biosynthesis is found together with antenna proteins in association with their biogenesis complex suggests that the folding of LHCPs upon insertion in the thylakoid membranes must be coupled with the integration of chlorophylls. However, it remains to be addressed whether this enzyme is functionally bound to Alb3.1 since other enzymes involved in the chlorophyll biosynthesis pathway were not detected in the Alb3.1 preparations.

cpSRP–Alb3.1 acts as an assembly apparatus of LHCPs

LC–MS/MS and immunoblot analyses indicate that eight LHCI proteins (LHCA1, 2, 3, 4, 5, 6, 8 and 9) and four LHCII proteins

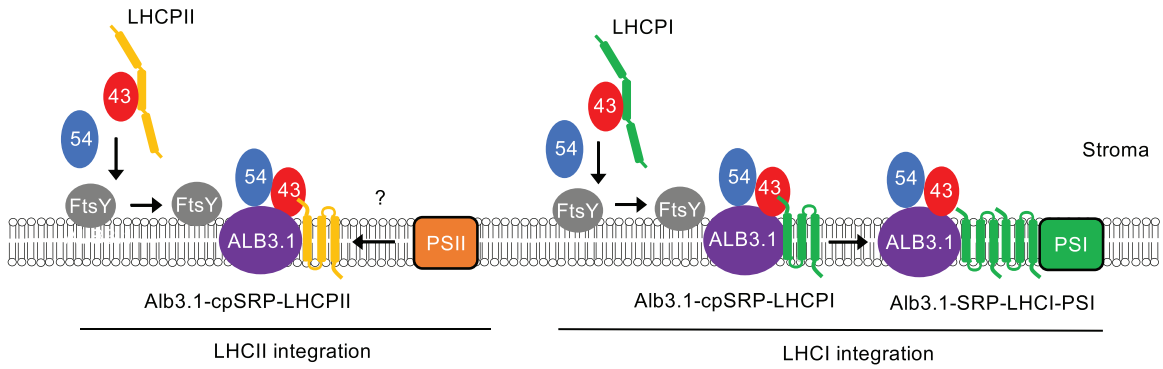

Fig. 5 A proposed model on the integration and assembly of green algal LHCPs. Two stromal factors, cpSRP43 and cpSRP54, may form a heterodimer (cpSRP). The cpSRP43 mainly binds LHCI and LHCII apoproteins in the stroma to form a transient cpSRP–LHCP complex, which is subsequently directed to the chloroplast SRP receptor protein FtsY on the stromal surface of the thylakoid membranes. Then the cpSRP–LHCP complex translocates the LHCP to Alb3.1 insertase by forming a cpSRP–Alb3.1–LHCP complex. The Alb3.1 assists insertion and assembly of LHCPs into the thylakoid membranes. The integrated LHCI polypeptides forms an LHCI oligomer and associates with the PSI core complex (Alb3.1–LHCI–PSI). Finally, the PSI–LHCI subcomplex is detached from Alb3.1. It remains elusive if the Alb3.1–LHCII–PSII subcomplex is formed because PSII–LHCII is looser than PSI–LHCI.

(LHCII types I and III, CP26 and CP29) are present in the purified Alb3.1–3HA preparation. The hydrophobic apoproteins of LHCs must associate with the cpSRP complex to remain soluble in the stroma and are targeted to the receptor cpFtsY and the insertase Alb3.1 to be integrated into the thylakoid membranes. Pulse-chase labeling experiments show that the LHCII types I and III proteins and probably CP26/29 bound to Alb3.1 are newly synthesized polypeptides (**Fig. 4**). The limited pulse-labeled signals of most LHCI proteins contrast with the significant labeling of LHCII proteins. This reflects the huge difference in the abundance of these two types of antenna, LHCII being synthesized rather actively, whereas the synthesis of LHCI proteins is relatively slow (Ozawa et al. 2010). Although LHCA7 and LHCII types II and IV are not detected in the Alb3.1–3HA preparation, it is highly likely that they also interact with the Alb3.1–cpSRP complex because the accumulation of LHCA7 and LHCII types II and IV is reduced to similar levels as the other LHC proteins in BF4 mutant cells. These proteins may be dissociated from the complex during the solubilization and/or purification procedures but the reason why the interaction of these proteins with cpSRP–Alb3.1 would be looser remains to be investigated.

It has been reported that the conserved L18 domain of LHC proteins, which consists of 18 amino acid residues and contains the crucial DPLG motif, binds to cpSRP43 proteins (Tu et al. 2000, Horn et al. 2015). The L18 domain is well conserved even in LHCII types II and IV. Although the L18 domain is less conserved in most LHCI proteins than in LHCII proteins, those of LHCA2, LHCA8 and LHCA9 are well conserved among nine LHCI proteins (Bujaldon et al. 2020). This suggests that the affinity between LHC proteins and the Alb3.1–cpSRP complex is not determined primarily by the extent of the conservation of the amino acid sequence of the L18 domain. Other regions of the LHC proteins may also be involved in the stable interaction with the Alb3.1–cpSRP complex.

Coupling between LHCI and PSI–LHCI assemblies

It is intriguing that PSI proteins (PsaA, PSAD and PSAF) were detected in the Alb3.1–3HA preparation, as shown in **Fig. 3**. This observation suggests that Alb3.1 is not only required for LHCI assembly but is also involved in the integration of LHCI complexes to a PSI core complex. It is also possible that Alb3.1 plays a role in a cotranslational insertion of the chloroplast-encoded PSI RC subunits (PsaA and PsaB) with 11 TM helices. Although the BF4 mutant accumulates PSI normally, there may be a redundant pathway assisted by Alb3.2 or other factors (Gohre et al. 2006). However, it remains to be addressed whether Alb3.1 and Alb3.2 is involved in the PSI RC assembly. **Fig. 5** shows a working hypothesis of how Alb3.1 is engaged in assembling LHCI complexes and the PSI–LHCI supercomplex. LHCI proteins translocated onto the stromal surface of the thylakoid membranes by the cpSRP complex would insert into the thylakoid membranes via Alb3.1. It remains unclear whether 10 LHCI complexes bind to a PSI core one by one. Alternatively, LHCI oligomers are first assembled, and the resulting oligomers are integrated into a PSI core to form a PSI–LHCI subcomplex. It is of interest that a PSI-deficient mutant accumulates oligomeric LHCI complexes consisting of inner and outer tetramers (Takahashi et al. 2004), suggesting that the oligomerization of LHCI complexes proceeds before the association to a PSI core. The Alb3.1–cpSRP complex would subsequently detach after the assembly of the PSI–LHCI subcomplex is completed. The association of the Alb3.1–cpSRP–LHCP complex with the PSI core may correspond to the large Alb3.1 complex of 600–700 kDa that we discussed above (Bellafiore et al. 2002).

In contrast, PSII proteins are not detected by immunoblotting, although PsbC (CP43) was detected by mass spectrometry (**Fig. 3** and **Table 1**). This inconsistency may result from the fact that mass spectrometry is generally more sensitive than immunoblotting. It is known that a dimer of the PSII

core complex associates with LHCII trimers and monomers (CP26 and CP29) to form a PSII–LHCII supercomplex (Shen et al. 2019, Sheng et al. 2021), but this supercomplex is much more unstable than PSI–LHCI supercomplexes. Thus, it is possible that the interaction between Alb3.1–cpSRP–LHCPs and a PSII core might be dissociated during the solubilization and purification procedures. It is of interest that the assembly of one of the PSII RC proteins, D1, is retarded in the *Alb3.1* deletion mutant ac29, and that reciprocal coimmunoprecipitation experiments suggested a direct or indirect interaction between Alb3.1 and D1 (Ossenbühl et al. 2004). Thus, it remains to be addressed if a transient complex between a PSII core complex and Alb3.1–cpSRP–LHCP complex is also formed.

Materials and Methods

Strains and culture conditions

WT and mutant strains of *C. reinhardtii* were grown in tris-acetate phosphate (TAP) medium at 25°C under continuous light of 50 μmol photons m^{-2} s^{-1} to the cell density of 2–5 × 10^6 cells ml^{-1}.

Plasmid construction and nuclear transformation

The DNA sequence of the *Chlamydomonas ALB3.1* gene was retrieved at GenBank (accession number: AF492768). Part of the *ALB3.1* coding region was amplified by nested polymerase chain reaction (PCR) (primers 1 and 2 for the first PCR, and primers 3 and 4 for the second PCR) using the *Chlamydomonas* cDNA library. The resulting PCR product was purified with the illustra GFX PCR DNA and Gel Band Purification Kit (GE Healthcare Life Science, Buckinghamshire), digested with *Nde*I and *Xba*I, and cloned into an *Nde*I/*Xba*I-digested pSL18 vector to generate plasmid pNK1. The pSL18 vector carries the paromomycin-resistant cassette and promoter/5′-UTR/terminator of the PSAD gene to drive foreign gene expression. The N-terminal coding region of *ALB3.1* was amplified by PCR with primers 5 and 6 using the *Chlamydomonas* cDNA library, and the resulting DNA fragment was inserted into an *Nde*I/*Pml*I-digested pNK1 with the In-Fusion HD Cloning Kit (Takara Bio Inc., Shiga) to generate pNK2. Annealed oligo DNAs from primers 7 and 8 were inserted into an *Eco*RI/*Xba*I-digested pUC18 vector to generate pSXY2002, which carries an HA tag coding region. Two sets of annealed oligo DNAs (primers 9 and 10 and primers 11 and 12) were simultaneously inserted into an *Eco*RI/*Xba*I-digested pUC18 vector to generate pSXY2004, which carries the triple HA tag coding region. The C-terminal coding region of *ALB3.1* was amplified by PCR using primers 13 and 14 and was then inserted into BstZ17I-digested pSXY2002 and pSXY2004 with the In-Fusion HD Cloning Kit to generate pMKR2 and pMKR3, respectively. Plasmids pMKR2 and pMKR3 were digested with *Mlu*I and *Xba*I and then cloned into an *Mlu*I/*Xba*I-digested pNK2 to generate pMKR4 and pMKR5, respectively. DNA segments amplified by PCR were confirmed by DNA sequencing.

Nuclear transformation was carried out by electroporation with an electroporator (Super Electroporator, NEPA21, typeII, Nepagene, Japan) basically as previously described (Nellaepalli et al. 2018) except that 10 μg/ml paromomycin instead of hygromycin was used for the selection of the transformants. BF4 cells grown in TAP medium were harvested at 600 × *g* and resuspended in TAP-sucrose solution to the density of 1 × 10^8 cells ml^{-1}. Plasmids pMKR4 and pMKR5 were digested by *Sca*I and introduced into BF4 cells. Insertion of the HA tag was confirmed by using PCR KOD FX Neo DNA polymerase (Toyobo, Tokyo) by using primers 15 and 16. The resulting PCR products were separated by 2.5% agarose gel electrophoresis, stained with ethidium bromide and visualized with a GelDoc Go Imaging System (BIO-RAD, Hercules, CA).

Oligo DNAs used in the present study are listed below.

1: 5′-AAGTCTTGGGTGATGCCCTGCAC
2: 5′-AACACGCAAACCACACGCATGCGCTG
3: 5′-GGGCATATGTACGTGCTGGCCGACGCCTCG
4: 5′-CCTCTAGAATCAAGCCGACGCACCGG
5: 5′-CACAACAAGCCCATATGTCGAGCTCCATGTGCCTGGCG
6: 5′-GTAGGAGTAGGGCACGTGCAGCTTGTCC
7: 5′-AATTCGTATACCCCTACGACGTGCCCGACTACGCCTAAT
8: 5′-CTAGATTAGGCGTAGTCGGGCACGTCGTAGGGGTATACG
9: 5′-AATTCGTATACCCCTACGACGTGCCCGACTACGCCTACCCCTACGACGT
10: 5′-GGGCACGTCGTAGGGGTAGGCGTAGTCGGGCACGTCGTAGGGGTATACG
11: 5′-GCCCGACTACGCCTACCCCTACGACGTGCCCGACTACGCCTAAT
12: 5′-CTAGATTAGGCGTAGTCGGGCACGTCGTAGGGGTAGGCGTAGTC
13: 5′-GATTACGAATTCGTAGATCTACCTGAAGAAGCTGGGCGG
14: 5′-CACGTCGTAGGGGTAAGCCGACGCACCGGCCACCGC
15: 5′-CAGCAAGGTGAACCGGCGCTGCAAGCGG
16: 5′-TCTCCATGGTACAGGCGGTCCAGCTGCTG

Thylakoid membrane reparation and affinity purification

Cells grown to the density of 5 × 10^6 cells ml^{-1} were collected by centrifugation (2,860 × *g* at 25°C for 5 min) and were resuspended in the buffer containing 25 mM HEPES-NaOH (pH 7.5), 1 mM $MgCl_2$ and 0.3 M sucrose. Cells were broken by the French Pressure Cell at 170–190 psi, and the thylakoid membranes were purified by the floating method using stepwise sucrose gradients as previously described (Chua and Bennoun 1975). Thylakoid membranes (400 μg Chl ml^{-1}) were solubilized with 1% α-DDM at 4°C for 10 min. The solubilized thylakoid extracts (500 μl) were incubated in a spin column followed by the addition of anti-HA beads (HA-tagged protein purification kit, MBL) for 1 h with constant end-over-end mixing. Nonadsorbed proteins to the HA beads in the column were removed by centrifugation (Nellaepalli et al. 2018). The columns were washed with the washing buffer (500 μl) 8–14 times. Alb3.1-HA and Alb3.1–3HA preparations were eluted two times with 20 μl elution buffer.

Pulse-chase labeling of proteins

Precultures from the cAlb3.1–1-HA strain were grown to a cell density of 2–3 × 10^6 cells ml^{-1} in 100 ml of the TAP medium containing reduced amounts of sulfur. The cells harvested by centrifugation were resuspended in TAP media containing no sulfur (25 μg Chl ml^{-1}) and were starved for sulfur under the light of 50 μmol photons m^{-2} s^{-1} for 2 h. Total cellular proteins were labeled with $Na_2{}^{35}SO_4$ (5 μCi ml^{-1}) (American Radiolabeled Chemicals) under the light of 50 μmol photons m^{-2} s^{-1} at 25°C for 20 min. The labeled proteins were chased by the addition of cold 10 mM Na_2SO_4 for 4 h. The radio-labeled cells were immediately subjected to thylakoid preparation as reported (Nellaepalli et al. 2018, 2021).

SDS-PAGE and Immunoblotting

Polypeptides from total cellular proteins, thylakoid membranes and affinity purified samples were separated by SDS-PAGE (Laemmli 1970, Fling and Gregerson 1986, Kashino et al. 2001). The separated polypeptides were visualized by staining with a fluorescent dye Flamingo (Bio-Rad, USA). Nitrocellulose membranes were used for blotting and probed with several antibodies raised against HA, PSI, PSII, LHCI and LHCII polypeptides. Immunoblotting signals were detected by enhanced chemiluminescence with a luminescent image gel analyzer (LAS-4000 mini, Fuji film). An antibody against HA was purchased from Medical & Biological Laboratories, Tokyo, Japan. Antibodies against PSI and LHCI subunits were described previously (Ozawa et al. 2018) and antibodies against LHCII subunits (Bujaldon et al. 2020) were described previously.

Antibodies against CP43 and D1 are a kind gift from Jean-David Rochaix and Masahiko Ikeuchi, respectively.

In-gel digestion and LC–MS/MS

In-gel tryptic digestion and following LC–MS/MS (LTQ, Thermofisher Scientific, USA) were performed as described in Ozawa et al. (2009). The acquired mass spectral data were analyzed with the Proteome Discoverer ver. 2.1.1.21 (Thermofisher Scientific, USA) against the protein database in ver. 5.5 Chlamydomonas genome of Joint Genome Institute for nuclear gene products and protein database in NC_005353 of National Center for Biotechnology Information for chloroplast gene products, respectively. Post-translational modifications were considered with dynamic modification: N-terminal acetylation, oxidation of tryptophan and methionine and phosphorylation of serine, threonine and tyrosine. A false discovery rate of 0.01 was calculated by the Decoy database search and filtered for all analyses.

Supplementary Data

Supplementary data are available at *PCP* online.

Data Availability

The data underlying this article are available in the article and in its online supplementary material.

Funding

JSPS KAKENHI (16H06554, 21H02510) to Y.T.

Disclosures

The authors have no conflicts of interest to declare.

References

Aldridge, C., Cain, P. and Robinson, C. (2009) Protein transport in organelles: protein transport into and across the thylakoid membrane. *FEBS J.* 276: 1177–1186.

Bellafiore, S., Ferris, P., Naver, H., Gohre, V. and Rochaix, J.-D. (2002) Loss of Albino3 leads to the specific depletion of the light-harvesting system. *Plant Cell* 14: 2303–2314.

Ben-Shem, A., Frolow, F. and Nelson, N. (2003) Crystal structure of plant photosystem I. *Nature* 426: 630–635.

Bujaldon, S., Kodama, N., Rathod, M.K., Tourasse, N., Ozawa, S.-I., Selles, J., et al. (2020) The BF4 and p71 antenna mutants from *Chlamydomonas reinhardtii*. *Biochim. Biophys. Acta* 1861: 148085.

Chua, N.H. and Bennoun, P. (1975) Thylakoid membrane polypeptides of *Chlamydomonas reinhardtii*: wild-type and mutant strains deficient in photosystem II reaction center. *Proc. Natl. Acad. Sci. U. S. A.* 72: 2175–2179.

Dall'Osto, L., Bressan, M. and Bassi, R. (2015) Biogenesis of light harvesting proteins. *Biochim. Biophys. Acta* 1847: 861–871.

DeLille, J., Peterson, E.C., Johnson, T., Moore, M., Kight, A. and Henry, R. (2000) A novel precursor recognition element facilitates posttranslational binding to the signal recognition particle in chloroplasts. *Proc. Natl. Acad. Sci. U. S. A.* 97: 1926–1931.

Dunschede, B., Bals, T., Funke, S. and Schunemann, D. (2011) Interaction studies between the chloroplast signal recognition particle subunit cpSRP43 and the full-length translocase Alb3 reveal a membrane-embedded binding region in Alb3 protein. *J. Biol. Chem.* 286: 35187–35195.

Dunschede, B., Trager, C., Schroder, C.V., Ziehe, D., Walter, B., Funke, S., et al. (2015) Chloroplast SRP54 was recruited for posttranslational protein transport via complex formation with chloroplast SRP43 during land plant evolution. *J. Biol. Chem.* 290: 13104–13114.

Fling, S.P. and Gregerson, D.S. (1986) Peptide and protein molecular weight determination by electrophoresis using a high-molarity tris buffer system without urea. *Anal. Biochem.* 155: 83–88.

Gohre, V., Ossenbuhl, F., Crevecoeur, M., Eichacker, L.A. and Rochaix, J.-D. (2006) One of two Alb3 proteins is essential for the assembly of the photosystems and for cell survival in Chlamydomonas. *Plant Cell* 18: 1454–1466.

Horn, A., Hennig, J., Ahmed, Y.L., Stier, G., Wild, K., Sattler, M., et al. (2015) Structural basis for cpSRP43 chromodomain selectivity and dynamics in Alb3 insertase interaction. *Nat. Commun.* 6: 8875.

Jeong, J., Baek, K., Kirst, H., Melis, A. and Jin, E. (2017) Loss of CpSRP54 function leads to a truncated light-harvesting antenna size in *Chlamydomonas reinhardtii*. *Biochim. Biophys. Acta* 1858: 45–55.

Jeong, J., Baek, K., Yu, J., Kirst, H., Betterle, N., Shin, W., et al. (2018) Deletion of the chloroplast LTD protein impedes LHCI import and PSI–LHCI assembly in *Chlamydomonas reinhardtii*. *J. Exp. Bot.* 69: 1147–1158.

Kashino, Y., Koike, H. and Satoh, K. (2001) An improved sodium dodecyl sulfate-polyacrylamide gel electrophoresis system for the analysis of membrane protein complexes. *Electrophoresis* 22: 1004–1007.

Kirst, H., Garcia-Cerdan, J.G., Zurbriggen, A. and Melis, A. (2012a) Assembly of the light-harvesting chlorophyll antenna in the green alga *Chlamydomonas reinhardtii* requires expression of the TLA2-CpFTSY gene. *Plant Physiol.* 158: 930–945.

Kirst, H., Garcia-Cerdan, J.G., Zurbriggen, A., Ruehle, T. and Melis, A. (2012b) Truncated photosystem chlorophyll antenna size in the green microalga *Chlamydomonas reinhardtii* upon deletion of the TLA3-CpSRP43 gene. *Plant Physiol.* 160: 2251–2260.

Laemmli, U.K. (1970) Cleavage of structural proteins during the assembly of the head of bacteriophage T4. *Nature* 227: 680–685.

Lewis, N.E., Marty, N.J., Kathir, K.M., Rajalingam, D., Kight, A.D., Daily, A., et al. (2010) A dynamic cpSRP43-Albino3 interaction mediates translocase regulation of chloroplast signal recognition particle (cpSRP)-targeting components. *J. Biol. Chem.* 285: 34220–34230.

Nellaepalli, S., Kim, R.G., Grossman, A.R. and Takahashi, Y. (2021) Interplay of four auxiliary factors is required for the assembly of photosystem I reaction center subcomplex. *Plant J.* 106: 1075–1086.

Nellaepalli, S., Ozawa, S.-I., Kuroda, H. and Takahashi, Y. (2018) The photosystem I assembly apparatus consisting of Ycf3–Y3IP1 and Ycf4 modules. *Nat. Commun.* 9: 2439.

Ossenbühl, F., Göhre, V., Meurer, J., Krieger-Liszkay, A., Rochaix, J.-D. and Eichacker, L.A. (2004) Efficient assembly of photosystem II in *Chlamydomonas reinhardtii* requires Alb3.1p, a homolog of Arabidopsis ALBINO3. *Plant Cell* 16: 1790–1800.

Ouyang, M., Li, X., Ma, J., Chi, W., Xiao, J., Zou, M., et al. (2011) LTD is a protein required for sorting light-harvesting chlorophyll-binding proteins to the chloroplast SRP pathway. *Nat. Commun.* 2: 277.

Ozawa, S., Nield, J., Terao, A., Stauber, E.J., Hippler, M., Koike, H., et al. (2009) Biochemical and structural studies of the large Ycf4-photosystem

I assembly complex of the green alga *Chlamydomonas reinhardtii*. *Plant Cell* 21: 2424–2442.

Ozawa, S., Onishi, T. and Takahashi, Y. (2010) Identification and characterization of an assembly intermediate subcomplex of photosystem I in the green alga *Chlamydomonas reinhardtii*. *J. Biol. Chem.* 285: 20072–20079.

Ozawa, S.-I., Bald, T., Onishi, T., Xue, H., Matsumura, T., Kubo, R., et al. (2018) Configuration of ten light-harvesting chlorophyll a/b complex I subunits in *Chlamydomonas reinhardtii* photosystem I. *Plant Physiol.* 178: 583–595.

Richter, C.V., Bals, T. and Schunemann, D. (2010) Component interactions, regulation and mechanisms of chloroplast signal recognition particle-dependent protein transport. *Eur. J. Cell Biol.* 89: 965–973.

Shen, L., Huang, Z., Chang, S., Wang, W., Wang, J., Kuang, T., et al. (2019) Structure of a C2S2M2N2-type PSII-LHCII supercomplex from the green alga *Chlamydomonas reinhardtii*. *Proc. Natl. Acad. Sci. U. S. A.* 116: 21246–21255.

Sheng, X., Liu, Z., Kim, E. and Minagawa, J. (2021) Plant and algal PSII–LHCII supercomplexes: structure, evolution and energy transfer. *Plant Cell Physiol.* In press.

Stengel, K.F., Holdermann, I., Cain, P., Robinson, C., Wild, K. and Sinning, I. (2008) Structural basis for specific substrate recognition by the chloroplast signal recognition particle protein cpSRP43. *Science* 321: 253–256.

Sundberg, E., Slagter, J.G., Fridborg, I., Cleary, S.P., Robinson, C. and Coupland, G. (1997) ALBINO3, an Arabidopsis nuclear gene essential for chloroplast differentiation, encodes a chloroplast protein that shows homology to proteins present in bacterial membranes and yeast mitochondria. *Plant Cell* 9: 717–730.

Takahashi, Y., Yasui, T., Stauber, E.J. and Hippler, M. (2004) Comparison of the subunit compositions of the PSI-LHCI supercomplex and the LHCI in the green alga Chlamydomonas reinhardtii. *Biochemistry* 43: 7816–7823.

Tu, C.J., Peterson, E.C., Henry, R. and Hoffman, N.E. (2000) The L18 domain of light-harvesting chlorophyll proteins binds to chloroplast signal recognition particle 43. *J. Biol. Chem.* 275: 13187–13190.

Ziehe, D., Dunschede, B. and Schunemann, D. (2017) From bacteria to chloroplasts: evolution of the chloroplast SRP system. *Biol. Chem.* 398: 653–661.

Ziehe, D., Dunschede, B. and Schunemann, D. (2018) Molecular mechanism of SRP-dependent light-harvesting protein transport to the thylakoid membrane in plants. *Photosyn. Res.* 138: 303–313.